HAL
open science

Iron and Fe–Mn mineralisation in Iran: implications for Tethyan metallogeny

Beate Orberger, Christiane Wagner-Raffin Wagner, Omar Boudouma, Colette Derré, Michel Fialin, Johan Neuville, Etienne Deloule, Ghasem Nabatian, Maryam Honarmand, Iman Monsef, et al.

To cite this version:

Beate Orberger, Christiane Wagner-Raffin Wagner, Omar Boudouma, Colette Derré, Michel Fialin, et al.. Iron and Fe–Mn mineralisation in Iran: implications for Tethyan metallogeny. Australian Journal of Earth Sciences, 2015, 62 (2), pp.211-241. 10.1080/08120099.2015.1002001 . hal-03521411

HAL Id: hal-03521411

https://hal.science/hal-03521411v1

Submitted on 11 Jan 2022

HAL is a multi-disciplinary open access archive for the deposit and dissemination of scientific research documents, whether they are published or not. The documents may come from teaching and research institutions in France or abroad, or from public or private research centers.

L'archive ouverte pluridisciplinaire **HAL**, est destinée au dépôt et à la diffusion de documents scientifiques de niveau recherche, publiés ou non, émanant des établissements d'enseignement et de recherche français ou étrangers, des laboratoires publics ou privés.

Iron-oxide ores in the Takab region, North Western Iran

Beate Orberger
GEOPS, Université Paris Saclay, Université Paris Sud, Bât 504, 91405 Orsay Cedex, France

Christiane Wagner, Omar Boudouma, Colette Derré, Michel Fialin
ISTeP and Centre Camparis, Sorbonne Université, UPMC Univ Paris 06, 4 Place Jussieu, 75005 Paris, France

Johan Neuville, Etienne Deloule
Centre de Recherches Pétrographiques et Géochimiques, CRPG, UMR 7358, CNRS-Université de Lorraine, F-54000 Vandoeuvre-lès-Nancy, France.

Ghasem Nabatian
University of Zanjan, Zanjan, Iran

Maryam Honarmand, Iman Monsef, Abdolreza Ghods
Institut of Advanced Studies of Basic Sciences, Zanjan, Iran

Abstract. The siliceous iron ore deposits in the NW part of Iran (Takab region) are hosted within para-metamorphic rocks, and are attributed to Late Proterozoic age. They comprise massive, banded, nodular and disseminated ore types, which are mainly composed of magnetite. Magnetite contains traces of Al. It is variously hematitized. Hematite show higher Al, Si and Ca contents than the magnetite. The iron oxides contain inclusions of zircons, apatite, uraninite, Mn-carbonate and euhedral monazite. Later hydrothermal solutions precipitated goethite surrounding the magnetite-hematite-maghemite grains and replacing hematite. Barite occurs in fractures of iron oxides, Mn-Ba-Pb oxi-hydroxides and scheelite occur interstitial to iron oxides. The ∂^{56}Fe values observed for magnetite decrease from disseminated to nodular iron ore (averages: +1.3, +0.4 and -0.4 ‰ (± 0.2 ‰), respectively). Iron isotopes of hematite in disseminated & layered ore show higher ∂^{56}Fe values than those of magnetite, in the range of +2 to +4 ‰ (± 0.2 ‰).

Key words: Iron ore Iran, iron isotopes, rare-earth elements

1 Introduction

Iran's yearly iron ore export reach about 23.5 million t. Over 90% is exported to China. Prediction up to until 2025, indicate that the iron ore production will triple, up to 66.2 Mt (Hastorun et al. 2016). Most of the iron deposits are located in the northeastern and central part of Iran, while iron ore deposits of the northwestern part are still little studied. Here we present results from the Takab Iron ore NW of Zanjan. Our study comprises mineralogy, geochemistry and Fe-isotope geochemistry.

2 Geological setting

In the Takab region, two tupes of iron ore deposits occur: (1) related to the Sanandaj-Sirjan Zone their formation may be related to the back-arc extension during the Prototethys subduction beneath the Cadomian magmatic arc (Ghorbani, 2013; Nabatian et al., 2015). (2) south of Takab, Meso-to Cenozoiciron oxide–apatite deposits Kiruna-type, are associated with plutonic rocks *(Nabatian 2012; Nabatian et al. 2013).* The latter present multiple vein deposits <1 000 t of iron ore. At present, the Morvarid & Sorkhe-Dizaj deposits (400 000 t) are mined.

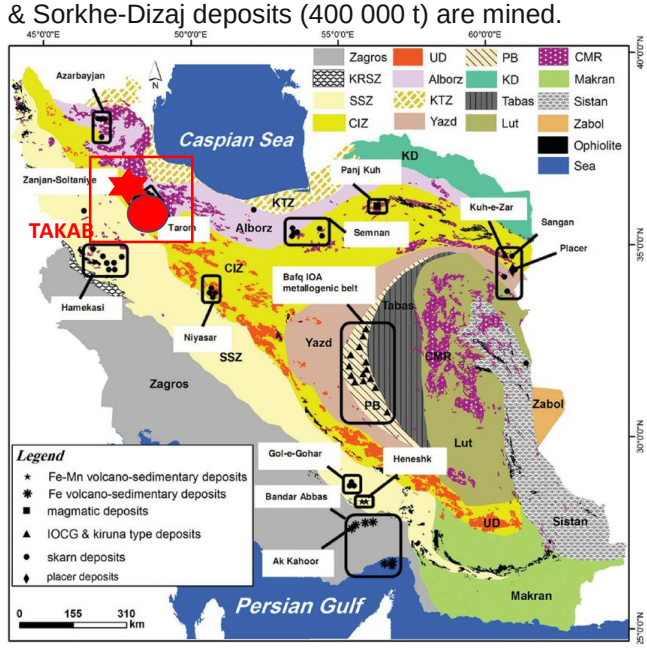

Figure 1. Tectonic and structural map of Iran (modified after Alavi 1991; Aghanabati 1998, 2005). The location of the study area is shown the red square, red star: volcano sedimentary iron ore, red dot: Kiruna type iron ores.

The mineralization forms thin layers and lenses interlayered with quartzite and amphibolites (Nabatian et al. 2015) In the study are, the iron oxide mineralogy is essentially described as hematite, goethite, with barite as accessory mineral. The age of the iron may be Late Proterozoic (Ghorbani et al., 2013).

3 Analytical Methods

Optical microscopy on polished thin sections was performed in transmitted and reflected light mode, SEM and electron microprobe analyses at the Centre Camparis, Sorbonne Université, UPMC Univ Paris 06, Paris, France. X-Ray Diffraction was carried out at GEOPS, Université Paris Saclay, Orsay, France. Iron isotope measurements were performed by SIMS at CRPG (Nancy), elemental geochemistry at SARM, CRPG, Nancy (XRF, ICP-MS).

4 Results

4.1 Petrology and Mineralogy

The studied samples are massive, banded and nodular iron ores. Disseminated ore is also present (Fig. 2 a, b, c). Massive, banded and nodular ore occur as decimetric layers within folded mica schist.

The host rocks of the massive magnetite are epidotized, amphibolitized chloritized fine grained plagioclase rich rocks, crosscut by veins of magnetite and carbonate. These rocks may represent metavolcanic rocks (basalts). X-ray diffraction on banded and nodular ore samples indicate that all samples contain similar major mineralogy quartz, magnetite, hematite, maghemite, goethite in different proportions. Small peaks are attributed to barite ($BaSO_4$). The magnetite and hematite host traces of Al (< 0.5 wt. %). Goethite hosts variable amounts of Al (up to 0.7 wt. %), Si (up to 1.7 wt. %) and Ca (up to 0.2 wt. %).

<u>The banded ore</u> shows coarse and discontinuous banding with interstitial quartz. Magnetite forms individual grains (~50 µm to several hundreds of µm), hosting detrital zircons (sometimes corroded) and droplet-like inclusions of PbS and ZnS. It is partly altered to hematite. Iron oxide veins occur perpendicular to the iron oxide bands. Goethite is abundant around hematized magnetite and in veins, sometimes hosting pyrite relics and P-bearing minerals. In the matrix, apart from quartz, Mn-Ba-oxides and barite (partly replacing Ba-feldspar (hyalophane)) and, rarely, uraninite occur. The matrix quartz grains show undulose extinction, indicating deformation.

<u>The nodular ore</u> is composed of mm-sized iron oxide agglomerates, partly elongated and disrupted in the quartz matrix (Fig. 2B). Other matrix minerals correspond to those in the layered ore. Magnetite is not hematized. It hosts inclusions of phosphates, Mn- and Fe- carbonates and uraninite.

<u>In the disseminated ore</u>, magnetite forms euhedral grains (~400 µm-1.5 mm), which are slightly hematized. The matrix minerals are quartz, minor K-feldspar and phengite. The feldspars host P (U, Th)-bearing phases, zircon and barite. Rutile, phosphates, scheelite, barite also occur interstitial to the matrix grains.

A

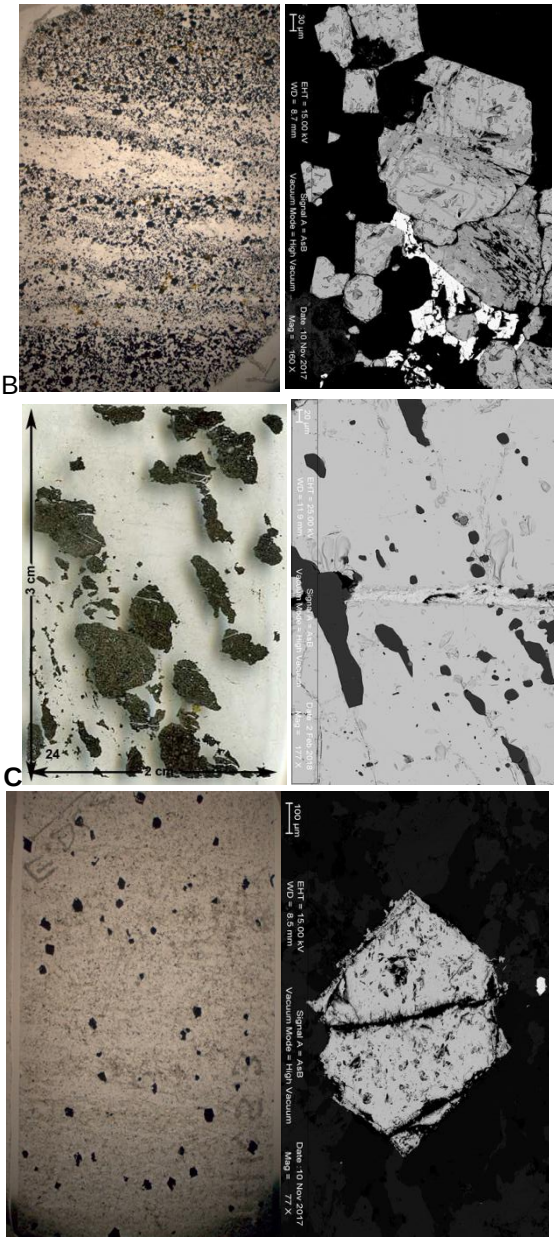

Figure 2. Polished thin section scans. A. Banded iron ore composed of alternating quartz and iron oxide bands and subhedral magnetite grains partly hematized; B. Nodular iron ore in quartz matrix, magnetite shows slight hematitization; C. Disseminated iron ore with euhedral magnetite grains

4.2 Geochemistry

The massive magnetite contains 77 wt.% total iron (Fe_2O_3) of which 22.52 wt. % of FeO. It is silica rich (14 wt.% SiO_2), and contains 1.7 wt.% Al_2O_3, 2,7 wt.% CaO and 0.35 wt.% CO_2. MnO and TiO_2 are low

(0.08 wt. % and 0.05 wt. %, respectively). Trace elements comprise 50 ppm Cu, 80 ppm Co, 88 ppm W, 14 ppm V, 25 ppm Sn, 40 ppm Zn and 30 ppm Zr are present. Arsenic and U are low (7 and 1 ppm respectively). The host rocks of the massive magnetite, the epidotized metabasalts contain about 54 wt.% SiO_2, 10 wt.% Al_2O_3, 9.8 wt. % total iron(Fe_2O_3), with two third FeO (.6 wt.%), 7.7 wt.% MgO, 8.8 wt.% CaO and 3.2 wt. % Na_2O. TiO_2 reaches 0.5 wt. %. Arsenic and U are as low as in the massive magnetite, however, the host rock is richer in Cr (270 ppm), Ni (70 ppm), V (132 ppm), Sc (25 ppm) Sr (170 ppm) and Ba (440 ppm).

The banded ore host variable iron contents (13-53 wt.% total Fe_2O_3, 0.56-12 wt.% FeO). Silica (SiO_2) ranges from 44 to 57 wt.%, Al_2O_3 from 0.08 to 0.33 wt.%. CO_2 contents are low, however S reaches up to 4.6 wt.% (barite). Barium is highest in this ore type (3300 ppm to about 15 wt.%). Traces such as As, Mo, V, Zn are also higher than in other ore types (≤80 ppm, ≤ 12 ppm, ≤ 84 ppm, ≤110, respectively).

The nodular ore is high in Fe_2O_3 (60 wt.%) and FeO (11 wt.%) and low in Al_2O_3 (0.1 wt.%). Pb, Zn (1000 ppm) and Cd (60 ppm) are higher than in other ore types. Ba is low (<2000 ppm), As and V similar than the other ore types. The disseminated ore is rich in SiO_2 (70-79 wt.% SiO_2), Total iron (Fe_2O_3) varies from 6 to 20 wt.% (0.9-4.6 wt.% FeO). Al_2O_3 reaches 14 wt.% in iron poor rocks, and is <0.2 wt.% in iron rich rocks. Arsenic reaches 31 ppm, while U is < 2 ppm. Barium contents range from 900 to 2450 ppm, Rb from 20 to 370 ppm, Zr from 50 to 250 ppm, V from 6 to 39 ppm and W from 38 to 122 ppm.

Rare-Earth-Element + Yttrium composition: PAAS normalized REE+Y patterns of the studied samples are shown in Fig. 2. All samples show a strong positive Y anomaly, and, except the massive magnetite and calcschist, a positive Eu anomaly. The massive magnetite shows a positive Ce anomaly and a strong enrichment in HREE compared to PAAS. The banded ores show variable REE/REE(PAAS) patterns. Most ore samples are characterized by an HREE enrichment and LREE depletion except for one banded ore (23). Banded and nodular ores shows both negative or an absence of Ce anomalies. The calcschist has a negative Ce anomaly. The Ba richest layered ore is poorest in LREE. The Y/Ho varies between 23.2 and 40. Highest values are observed in nodular ores (24: 40,4) and calcschist (35: marble (1,2)), most oscillate around values typical for shales (25-27).

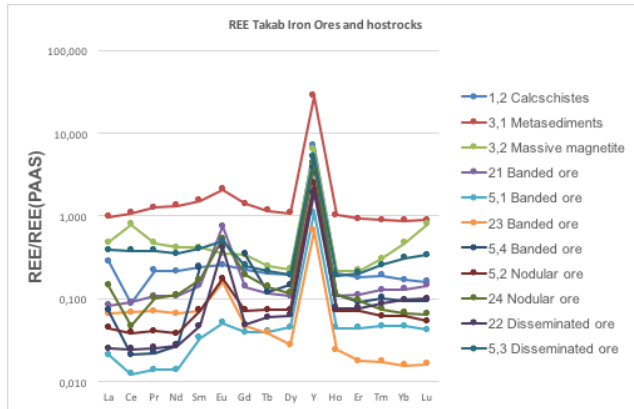

Figure 3. REE/REE(PAAS)- normalized patterns of the studied samples.

4.3 Iron- and oxygen isotope Geochemistry

All ore types were analyzed for ∂^{56}Fe (Fig. 4). In the banded ore, the magnetite is characterized by ∂^{56}Fe (-0.3 to +1 ‰ ± 0.2 ‰) and variable ∂^{18}O (-2 to +2 ‰).

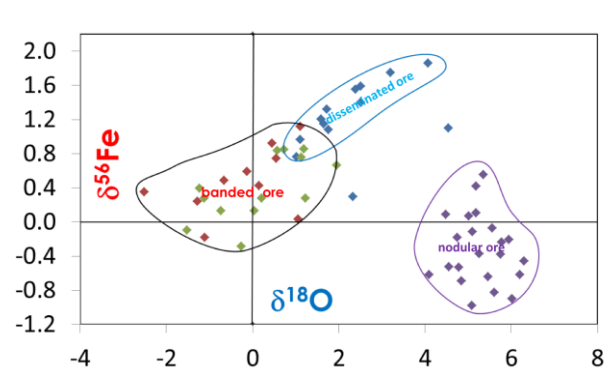

Figure 4: d^{56}Fe versus d^{18}O (‰) of the studied samples.

In the nodular ore, the magnetite is characterized by ∂^{56}Fe (-1 to +0.5 ‰ ± 0.2 ‰) and ∂^{18}O between +4 to +6 ‰. In the disseminated, the magnetite is characterized by ∂^{56}Fe (+0.7 to +2 ‰ ± 0.2 ‰) and ∂^{18}O between 0.5 ‰ and +4 ‰.

The ∂^{56}Fe values observed for magnetite decrease from disseminated to nodular iron ore (averages: +1.3, +0.4 and -0.4 ‰ (± 0.2 ‰), respectively). Iron isotopes of hematite in disseminated and layered ore show higher ∂^{56}Fe values than those of magnetite, in the range of +2 to +4 ‰ (± 0.2 ‰).

5 Discussion and Conclusions

Petrological and mineralogical studied (Orberger et al. 2017 showed that that primary magnetite ore is banded and crystallized statically from an iron and silica rich solution. Zircon, apatite, Mn-carbonates, uraninite and monazite were included during this step in the initial iron oxide, magnetite. Based on REE + Y

compositions it can be conclude that reducing seawater with a contribution from hot hydrothermal solutions is the source of magnetite ores.

Regional deformation is indicated by grain boundary migration during the recrystallization of quartz grains. The nodular ore represents most likely a highly deformed banded iron ore, where magnetite bands were disrupted and recrystallized. Sulphides were present at that state. Oxidizing fluids accompanied this step and transformed the magnetite into maghemite and hematite. (3) Aqueous solutions carrying Mn, Ba, Pb, Ca, W, S, CO_2 led to the formation of goethite and Mn-Ba-Pb oxi-hydroxides and associated scheelite and barite. This episode is most likely contemporaneous to the W mineralisation in this region (Ghorbani, 2013).

This scenario is supported by increasing ∂^{56}Fe and ∂^{18}O with progressive oxidation from banded, nodular to disseminated magnetite reaching highest values in hematite (Orberger et al.2018). A shift in ∂^{56}Fe towards positive values in oxidizing environments was also observed for example by Rouxel et al (2008).

Acknowledgements

We thank the Institute of Advanced Sciences of Basic Science and University of Zanjan, Zanjan for logistic support during fieldwork and the stay of BO in Zanjan. Campus France and the French embassy (Gundishapur program 2017-2019) are thanked for financing the stay of BO at IASBS, Zanjan. The UMR7193 ISTeP, UPMC is thanked for financial support of the analyses.

References

Aghanabati A. 1998. Major sedimentary and structural units of Iran (map). Geosciences, 7, 29-30.

Aghanabati A. 2005. Geology of Iran. Geological Survey of Iran (Persian book), Tehran, Iran, 538 pp.

Alavi M. 1991. Sedimentary and structural characteristics of the Paleo-Tethys remnants in northeastern Iran. Geological Society of America Bulletin, 103, 983-992.

Hastorun S, Renaud KM, Lederer GW (2016) Recent trends in the nonfuel minerals industry of Iran: U.S. Geological Survey Circular 1421, 18, http://dx.doi.org/10.3133/cir1421.

Ghorbani M. (2013) The Economic Geology of Iran: Mineral Deposits and natural Ressources. Springer Dordrecht Heidelberg New York, 567. ISBN 978-94-007-5624-3 ISBN 978-94-007-5625-0 (eBook), DOI 10.1007/978-94-007-5625-0.

Nabatian Gh. 2012. Geology, geochemistry and evolution of ironoxide apatite deposits in the Tarom volcano-plutonic belt, western Alborz. Unpublished PhD thesis, Tarbiat Modares University, Tehran, Iran, 375 pp.

Nabatian Gh., Ghaderi M., Dalirian F. & Rashidnejad-Omaran, N. 2013. Sorkhe- Dizaj iron oxideapatite ore deposit in the CenozoicAzarbaijan magmatic belt, NW Iran. Resource Geology 63, 4256.

Nabatian G., Rastad F, Neubauer F, Ghaderi, M (2015) Iron and Fe–Mn mineralisation in Iran: implications for Tethyan metallogeny. Australian Journal of Earth Sciences, 62:2, 211-241, DOI: 10.1080/08120099.2015.1002001

Rouxel, O, Shanks, W.C., Bach, W., Edwards, K.J. 2008., Integrated Fe-and S isotopes study of seafloor hydrothermal vents at East Pacific Rise 9-10°. Chemical Geology 252, 214-227. DOI: 10.1016/j.chemgeo.2008.03.009